Evaluation of an Immortalized Retinal Endothelial Cell Line as an *in Vitro* Model for Drug Transport Studies across the Blood-Retinal Barrier

Jie Shen,[1,2] Stacy T. Cross,[1] Diane D. S. Tang-Liu,[1] and Devin F. Welty[1]

Received January 7, 2003; accepted May 15, 2003

Purpose. To evaluate the growth and barrier properties of an immortalized rat retinal endothelial cell line (TR-iBRB) maintained on permeable membrane for drug transport studies.

Methods. TR-iBRB cells were grown on permeable membrane filters. The effect of coating material on cell growth was investigated. Transport of [^{14}C]-3-O-methyl-D-glucose (3-OMG), AGN 194716, AGN 195127, AGN 197075, acebutolol, alprenolol, atenolol, brimonidine, carbamazepine epoxide (CBZ-E), metoprolol, nadolol, rhodamine 123, and sotalol was measured across the cultured cell layer to determine the apparent permeability coefficients (P_{app}). Rhodamine 123 uptake into these cells in the presence of these test compounds was evaluated. Western blot was performed to detect the efflux transporter P-glycoprotein (P-gp). Bidirectional transport in MDR1-MDCK cell monolayers overexpressing the human P-gp was measured for AGN 197075.

Results. TR-iBRB cells form confluent cell layers when grown on fibronectin-coated membrane and exhibit characteristic spindle-shaped morphology. A good correlation between P_{app} and cLogD (pH 7.4) of the compounds tested was observed, except for 3-OMG, AGN 197075, and rhodamine 123, which are substrates of carrier-mediated transport systems such as P-gp and a glucose transporter (GLUT1). When grown on permeable membrane, TR-iBRB cells expressed functional P-gp and GLUT1.

Conclusions. TR-iBRB cells, when grown on permeable membrane, provide a useful tool for predicting permeability across the BRB. The usefulness of this model for high-throughput screening and rank ordering of drug candidates intended for the back of the eye in treatment of ocular diseases needs further characterization upon correlation with *in vivo* data.

KEY WORDS: blood–retinal barrier (BRB); cell culture; immortalized; transport; permeability.

INTRODUCTION

Many ocular diseases involve pathologic conditions of the retina. Glaucoma patients suffer from progressive vision loss caused by damaged retinal ganglion cells as a result of elevated intraocular pressure. Retinal neovascularization and the resulting vascular hyperpermeability cause vision loss in diabetic retinopathy (1). In the case of infectious diseases, especially in the acquired immunodeficiency syndrome (AIDS) patient population, the infection may affect retina or the posterior portion of the eye and lead to sudden vision loss (2). Retinitis pigmentosa involves disturbances in retinal metabolism, pigment clumping at the site of the retinal pigment epithelium, and is manifested by progressive visual field loss, night blindness, and abnormal electroretinogram (3). These ocular diseases warrant effective drug delivery to the retina and/or the posterior segment of the eye.

From a systemic drug delivery perspective, retina drug delivery may be improved by modification of blood-retinal barrier (BRB) permeability, chemical modification of the drug for better BRB penetration, and liposome encapsulation or coupling of the drug to specific vectors. The BRB is well known to be a particularly tight barrier, similar to the blood–brain barrier (BBB), and responsible for homeostasis of the neuroretina (4). The BRB consists of the outer barrier in the retinal pigment epithelium and an inner barrier in the endothelial membrane of the retinal capillary vessels. Retinal capillary vessels differ from vessels in other parts of the body (except those in the brain) in that their intercellular junctions demonstrate extensive "zonulae occludentes," which completely seal the intercellular space of the endothelium (5).

Several laboratories have developed various *in vitro* models of the inner BRB to understand transport processes across these endothelial cell layers (6–8). Compared to *in vivo* animal models, *in vitro* models manage to avoid the complex anatomic structure and inaccessibility of the retina for delineation of drug transport. Recently, a transgenic rat model harboring the temperature-sensitive SV40 large T-antigen gene was used to develop an immortalized rat inner BRB cell line named TR-iBRB cells by Hosoya *et al.* (9). TR-iBRB cells become immortalized and grow rapidly when maintained at 33°C.

The main advantage of an immortalized retinal capillary endothelial cell line over primary cell culture is obviation of the experimental complexity of harvesting cells from source tissues as small as the retina capillaries and the requirement to be freshly isolated from animals. Moreover, primary cell cultures are typically more susceptible to heterogeneity in cell population, which introduces greater variability across studies. Therefore, very few transport studies using primary cultured retinal endothelial cells have been reported. The TR-iBRB cells, being an immortalized cell line derived specifically from purified retinal endothelium (9), may serve as a useful tool to investigate drug transport at the inner BRB.

The purpose of this study was to grow the TR-iBRB cells on a permeable membrane, characterize the cell layer development, and evaluate the cell culture for permeability measurements to predict transport across the inner BRB.

MATERIALS AND METHODS

Materials

Fetal bovine serum (FBS), antibiotic-antimycotic 100× cocktail (penicillin, streptomycin, and amphotericin B), Dulbecco's modified Eagle's medium (DMEM) low glucose, Dulbecco's phosphate-buffered saline, and trypsin-EDTA were purchased from Invitrogen Life Technologies (Carlsbad, CA). Bovine endothelial cell growth factor (bECGF) was purchased from Roche Applied Science (Indianapolis, IN). Cell-freezing media were obtained from Sigma (St. Louis, MO). Collagen type I-coated cell culture flasks and recombi-

[1] Department of Pharmacokinetics and Drug Metabolism, Allergan, Inc., Irvine, California 92612.

[2] To whom correspondence should be addressed. (e-mail: shen_jie@allergan.com)

nant human fibronectin were purchased from BD Sciences (Bedford, MA). Transwell™ plates and 12-well cluster dishes were purchased from Costar (Cambridge, MA).

Cell Culture

TR-iBRB cells were obtained from YS New Technology Institute, Inc. (Tochigi, Japan) and were used between passages 22 and 50. Cell growth media consisted of DMEM low-glucose media supplemented with 10% FBS, 1× antibiotic-antimycotic, and 15 μg/ml bECGF. Cell stock was grown in type I collagen-coated cell culture flasks in a 5% CO_2 humidified chamber at 33°C. For cells grown on Transwell™ filters, cells were seeded at 2×10^5 cells/cm^2. Membrane coating material as cell substrata including collagen, fibronectin, matrigel, and gelatin were tested for optimal cell growth. Morphologic characterization was carried out to determine the choice of membrane coating material for subsequent cell cultures.

P-gp–transfected Madin-Darby Canine Kidney (MDR1-MDCK) epithelial cells were obtained from Dr. Piet Borst at the Netherlands Cancer Institute (Amsterdam, Netherlands) and were used between passages 13 and 29. Cell growth media consisted of DMEM high-glucose media supplemented with 50 U/ml penicillin, 50 μg/ml streptomycin, and 10% FBS. Cells were grown in a 5% CO_2 humidified chamber at 37°C.

Transepithelial (transendothelial) electrical resistance (TEER) values were measured across cell layers grown on Transwell™ membrane filter using Endohm™ resistance meter (WPI, Sarasota, FL). The reported TEER values were calculated by subtracting TEER values of blank filters from the direct measurement of TEER for cell layers grown on filters.

Transport Studies in TR-iBRB Cells

For transport experiments, TR-iBRB cells were seeded on fibronectin-coated Transwell™ filters at 2×10^5 cells/cm^2 and grown for 3 days, at which time cell layers became confluent. To assess the permeability barrier property of the endothelial cell layer, transport of [^{14}C]-3-O-methyl-D-glucose (3-OMG), AGN 194716, AGN 195127, AGN 197075, acebutolol, alprenolol, atenolol, brimonidine, carbamazepine epoxide (CBZ-E), metoprolol, nadolol, rhodamine 123, and sotalol across the cell layer was measured. Briefly, a total of 200 μl dosing solution (10 μM test compound) was applied to the apical side of the cell layer, while the basolateral side was bathed in 800 μl unsupplemented DMEM low-glucose medium as the transport buffer. At 2, 5, 10, 20, 40, and 60 min postdose, aliquots of 400 μl fluid were sampled from the basolateral compartment and analyzed by either a liquid scintillation counter, fluorescence spectrophotometer, or LC-MS/MS. Each time after sampling, 400 μL of fresh transport buffer was immediately added back to the basolateral compartment to maintain a "sink" condition, and the fluids were mixed by pipetting up and down at least three times. Transport of all compounds was also measured across blank fibronectin-coated Transwell™ filters to access the barrier property presented by the filter alone. Unless otherwise indicated, four filters with or without cell layers were used in transport studies of each compound.

To obtain a transport parameter, clearance was calculated for each compound. The increment in cleared volume between successive samplings was calculated by dividing the amount of solute transported during the interval by the donor solution concentration. The total volume cleared at each time point was calculated by summing the incremental cleared volumes up to the given time point,

$$\text{Clearance } (\mu L) = [C]_R \times V_R/[C]_D \quad (1)$$

where $[C]_R$ is the sampled receiver solution concentration, V_R is the receiver compartment volume, and $[C]_D$ is the donor solution concentration. During the 60-min experiment, the clearance volume increased linearly with time. The average cleared volume was plotted vs. time, and the slope was estimated by linear regression analysis (Microsoft Excel™ 97). The slope of the clearance curves for cell layers grown on filter was denoted PS_t, where PS is the permeability–surface area product in μl/min. The slope of transport across blank filter was denoted PS_f. The PS value for TR-iBRB cell layers (PS_e) was subsequently calculated from

$$1/PS_e = 1/PS_t - 1/PS_f \quad (2)$$

The PS_e values were divided by the surface area of the filter membrane to generate the permeability coefficient P_{app} (cm/s) for the TR-iBRB cell layer. The octanol–water partition coefficients of all tested compounds as partially dissociated at pH 7.4 (cLogD) were calculated using ACD/LogD Suite™ (version 5.15, Advanced Chemistry Development, Toronto, Canada).

Uptake Experiments

Uptake of rhodamine 123, a known P-gp substrate, was carried out in TR-iBRB cells grown in 12-well cluster dishes, in the presence and absence of AGN 194716, AGN 195127, AGN 197075, acebutolol, alprenolol, atenolol, brimonidine, carbamazepine epoxide (CBZ-E), metoprolol, nadolol, and sotalol.

For all uptake experiments, cells were grown to confluency as determined by light microscopy. The growth medium was first aspirated off, and the cells were preequilibrated in fresh transport buffers (DMEM low glucose) at 37°C for 30 min. The cell layers were then equilibrated at 37°C for 30 min either in transport buffer (control) or in transport buffers containing test compounds (at 1 mM). Uptake of rhodamine 123 (10 μM) was then measured at 37°C for 2 h in the absence (control) and presence of test compounds (at 1 mM). At the end of the experiments, dosing solutions were removed, and the cell layers were rinsed three times with ice-cold stop solution (PBS containing 0.1% w/v sodium azide). The cell layers were then solubilized on an orbital shaker (200 rpm) for 1 h by lysing solution (0.5% v/v Triton X-100 in 0.2 M NaOH). Fluorescent level of the cell lysate was determined by Fluostar Galaxy (BMG Labtechnologies, Durham, NC) at excitation/emission wavelengths of 485/520 nm. Autofluorescence of untreated cells was also measured and subtracted from that of cells incubated with rhodamine 123. The amount of intracellularly accumulated rhodamine 123 was quantified against a standard curve of rhodamine 123 in lysing solution (from 0.01 to 2.0 μM).

The protein content of each cell layer was determined by the DC protein kit (Biorad Laboratories, Hercules, CA) to

normalize for cell number. Uptake data were expressed as percent of rhodamine 123 accumulation compared to control.

Western Blot Analysis

Cell membrane protein was prepared for Western blot analysis. TR-iBRB cell layers grown in type I collagen-coated cell culture flasks and fibronectin-coated Transwell™ filters were scraped off and resuspended in MSEP solution (125 mM mannitol, 40 mM sucrose, 1 mM EDTA-Tris, and 5 mM PIPES-Tris) containing protease inhibitor cocktail (Sigma, St. Louis, MO). After homogenization, the cell homogenate was centrifuged at 1000 × *g* for 10 min. The supernatant was further centrifuged at 367,000 × *g* at 4°C for 15 min and the pellets resuspended with MSEP for further analysis. The same procedure was carried out for MDR1-MDCK cells grown in cell culture flasks and on Transwell™ filters to serve as the positive control. Protein quantification was carried out by the DC protein assay. The isolated membrane protein (60 μg) was electrophoresed on SDS-polyacrylamide gel (7.5% Tris-HCl Bio-Rad Precast Gel) and subsequently electrotransferred to a Hybond membrane (Amersham Biosciences). Primary mouse monoclonal C219 anti P-gp antibody (Signet, Dedham, MA) and secondary goat-antimouse antibody (Bio-Rad) were used to detect P-gp. The immunoblot procedure using the enhanced chemiluminescence method (ECL) was performed (Immun-Star chemiluminescent kit, Bio-Rad).

P-gp Functional Study Using MDR1-MDCK Cells

MDR1-MDCK cell layers grown on noncoated Transwell™ filter were used to measure AGN 197075 transport in the apical to basolateral (A to B) and basolateral to apical (B to A) directions. The A to B transport was carried out as described above for transport in TR-iBRB cells. For B to A transport, 800 μl dosing solution was placed at the basolateral side of the cell monolayer, and 100-μl samples were taken from a total of 200 μl apical fluid at 2, 5, 10, 20, 40, and 60 min postdose. Apical fluid was replenished with 100 μl fresh transport buffer after each sampling point. Samples were analyzed using a liquid chromatography tandem mass spectrometry method (LC-MS/MS).

RESULTS

Morphologic and Bioelectrical Characterization of Cell Layers Grown on Permeable Membrane

TR-iBRB cells exhibit the endothelial characteristic spindle-fiber-shaped morphology when grown on rat tail collagen type I-coated tissue culture flasks (9). When the cells were seeded on permeable membrane of Transwell™ filters, their morphologic development is dependent on the subcellular matrix coated on the membrane. On noncoated and gelatin-coated filter membrane, the cells adopt a "cobblestone" appearance with distinct cell borders (Fig. 1). On matrigel-coated membrane, the cells clearly formed multiple cell layers with a thin fibrous appearance. When the membrane filter was coated with type I collagen, the cells aggregated and did not form confluent cell layers as they did on other matrices. Only when the membrane was coated with recombinant human fibronectin did the cells assume the spindle-fiber-shaped morphology similar to that observed when they are grown on solid support as well as to primary cell culture of the bovine brain endothelial cells (10).

However, the cell layers failed to form tight barriers as gauged by their TEER values on any type of subcellular matrix (Fig. 2). The TEER values plotted reflect the difference between TEER of cell layers grown on filters and that of bare filters with corresponding coating material. Over 5 days of cell culture, TEER values typically climbed slowly (except for cells grown on collagen-coated filter) and plateued 4 days postseeding at lower than 30 $\Omega \cdot cm^2$. Among the five different subcellular matrices, only TEER values measured for cell layers grown on collagen-coated filters were statistically different from others ($p < 0.05$).

Transport across TR-iBRB Cells

A typical result for a transport experiment using four filter inserts coated with human fibronectin with and without

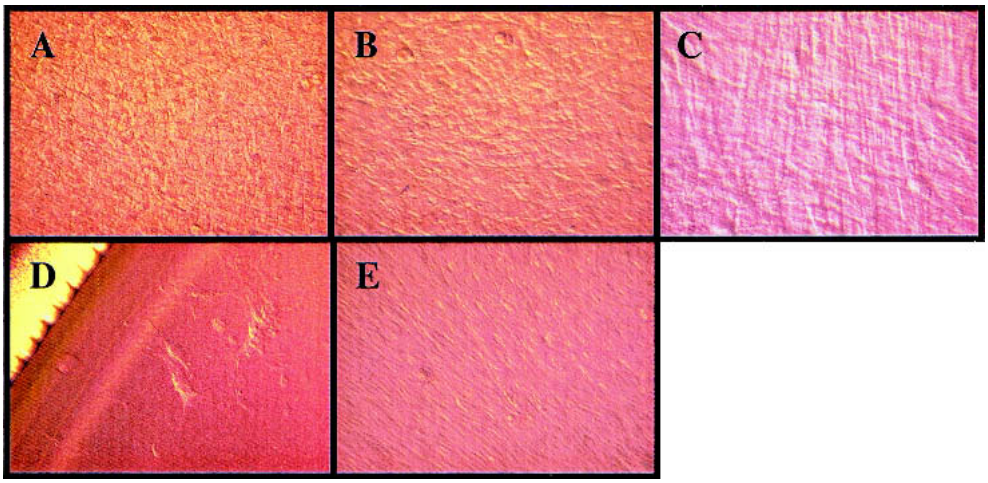

Fig. 1. Phase-contrast micrographs of TR-iBRB cells grown on (A) noncoated polyethylene Transwell™ filter; (B) gelatin-coated filter; (C) matrigel-coated filter; (D) type-I collagen-coated filter; and (E) human fibronectin-coated filter (×100 magnification).

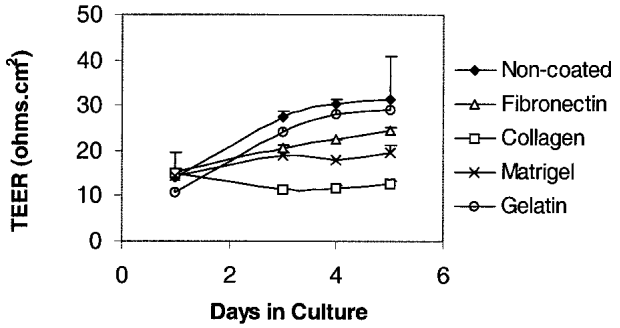

Fig. 2. Time course of TEER development for TR-iBRB cells cultured on permeable membrane filter with different subcellular matrix coating. Cells were seeded at 2×10^5 cells/cm^2. Each data point represents mean ± SD for n = 3.

TR-iBRB cell layer is shown in Fig. 3. The slopes of clearance over time were linear during the 60-min experiment for all compounds. P_{app} values for the tested compounds are listed in Table I. Only compounds with greater than 80% of recovered dose were included in the table. Also listed are cLogD values for each compound. The P_{app} values were plotted against their cLogD values and shown in Fig. 4. A linear correlation (r = 0.82) was observed for 10 of the 13 compounds tested.

P-gp Expression and Function in TR-iBRB Cells

Western blot analysis by C219 monoclonal antibody of membrane protein harvested from TR-iBRB cells and MDR1-MDCK cells grown both on Transwell™ filter membrane and in cell culture flask is shown in Fig. 5. The protein detected for TR-iBRB cells had a molecular weight of ~170 kDa, as expected for P-gp. The protein detected for MDR1-MDCK cells had the same molecular weight.

Rhodamine 123 uptake into TR-iBRB cells in the presence and absence of test compounds identified AGN 197075 as an inhibitor of P-gp-mediated efflux of rhodamine 123, whereas all other compounds did not exhibit such an inhibitory effect (Fig. 6). In addition, AGN 197075 was transported preferentially in the basolateral to apical direction than in the opposite direction when its bidirectional transport was measured in confluent MDR1-MDCK cell monolayers (P_{app}BA/P_{app}AB ratio > 4, Fig. 7).

DISCUSSION

Hosoya *et al.* (9) demonstrated that TR-iBRB cells in culture express the glucose transporter GLUT1 as well as

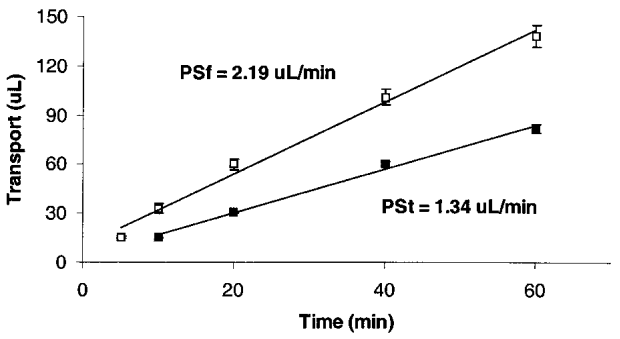

Fig. 3. Clearance of atenolol across cultured TR-iBRB cell layers (■) or across blank filters coated with human fibronectin (□) in 60 min. Data represent mean ± SEM (n = 4).

Table I. Permeability Coefficient (P_{app}) across Cultured TR-iBRB Cell Layers

Compounds	M.W.	$cLogD_{7.4}$	$P_{app} \times 10^5$ (cm/s)
3-O-Methyl-D-glucose	194	–2.67	6.00
AGN 194716	232	1.76	15.9
AGN 195127	230	1.54	13.4
AGN 197075	263	1.26	6.50
Acebutolol	336	0.41	6.00
Alprenolol	249	1.13	10.4
Atenolol	266	–1.66	5.10
Brimonidine	292	–0.49	3.90
CBZ-E	252	0.69	15.8
Metoprolol	267	0.026	4.80
Nadolol	309	–0.47	7.90
Rhodamine 123	344	2.13	1.35
Sotalol	272	–1.46	2.80

P-gp by Western blot. Additional functional data for GLUT1 were presented via saturable uptake of its substrate 3-OMG in the TR-iBRB cells. Both GLUT1 and P-gp have been shown to exist in the inner BRB (6,11). More recently, the same authors demonstrated the presence of the monocarboxylate transporter 1 (MCT1) in TR-iBRB cells by reverse transcription polymerase chain reaction (RT-PCR) and functional assay of L-lactic acid transport (12). MCT1 has also been identified *in vivo* in the inner and outer BRB to facilitate transport of lactic acid and other monocarboxylates such as pyruvate and the ketone bodies between the retina and the blood (13). Therefore, it appears that this immortalized cell line retains several active transporter systems identified at the BRB *in vivo*. The purpose of the present study was to evaluate TR-iBRB cells, when grown on permeable membrane, as a potential model for the inner BRB for high-throughput drug permeability screening.

One major challenge faced by researchers attempting to develop *in vitro* models of the BBB and BRB using endothelial cell culture is to attain cell layers with the same tightness as that observed *in vivo*. Many laboratories throughout the world have made significant efforts to establish such models.

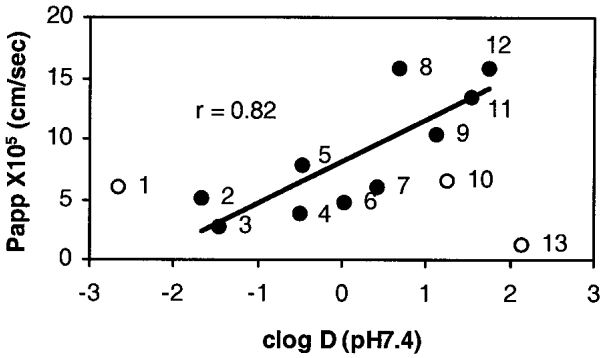

Fig. 4. Influence of lipophilicity (as estimated by cLogD values) on permeability coefficient (P_{app}) across TR-iBRB cell layers. Linear regression was generated using filled data points. Key: (1) 3-O-methyl-D-glucose; (2) atenolol; (3) sotalol; (4) brimonidine; (5) nadolol; (6) metoprolol; (7) acebutolol; (8) CBZ-E; (9) alprenolol; (10) AGN 197075; (11) AGN 195127; (12) AGN 194716; (13) rhodamine 123. Data represented by closed symbols were used to construct the linear regression.

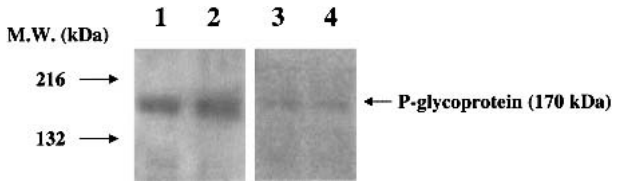

Fig. 5. Western blot analysis of P-gp expression in MDR1-MDCK and TR-iBRB cell membrane. Lane 1: MDR1-MDCK cells grown on Transwell™ membrane. Lane 2: MDR1-MDCK cells grown in cell culture flask. Lane 3: TR-iBRB cells grown on Transwell™ membrane. Lane 4: TR-iBRB cells grown in cell culture flask.

However, the highest reported TEER values for these cultured cells were in the range of 400–700 $\Omega \cdot cm^2$ for primary cultured bovine and porcine brain microvessel endothelial cells (14,15). Typically the TEER values are below 300 $\Omega \cdot cm^2$ for these endothelial cell cultures, whether cultured alone or cocultured with astrocytes (16,17). In this regard, the immortalized TR-iBRB cells used in the present study were consistent with previously reported models (Fig. 2), despite the fact that numerous culture conditions including culture media, subcellular matrix, and seeding density were tested. Of these conditions, the cells grown on fibronectin-coated filter membrane manifested similar morphology to that characteristic of endothelial cells in primary cell culture (Fig. 1). Moreover, TR-iBRB cell layers were able to differentiate permeability of compounds with a range of hydrophilicity as well as those transported by active mechanisms.

It has been well established that drug distribution into the brain occurs more readily for lipophilic compounds than for hydrophilic ones (18), and for compounds that passively diffuse across biologic barriers, there is a good correlation between BBB permeability and their physicochemical properties including lipophilicity and molecular weight (19). Because compounds tested in the current study have similar molecular weight, we evaluated the correlation between TR-iBRB cell layer permeability and compound lipophilicity as gauged by cLogD values (Table I and Fig. 4). The cLogD values were estimated instead of the octanol–water partition coefficient (LogP) values conventionally used because they take into account the ionization of compounds at neutral pH, at which transport experiments were carried out. The cLogP estimation, on the other hand, can be accurately performed only for uncharged substances. The cLogD estimation incorporates prediction of both the acid-base ionization coefficient, pK_a, and cLogP, and therefore provides a more accurate estimation of lipophilicity for compounds that are ionizable at neutral pH. Our results show that the TR-iBRB cells were able to differentiate compounds with different lipophilicity with cLogD in the range between approximately –2 and 2 (Fig. 4), the more lipophilic compounds being more permeable across the cell layers. A similar relationship was observed for a wide range of compounds when *in situ* brain perfusion was conducted in rats and mice (20), and when brain uptake of intravenously injected radiolabeled compounds was measured in rats (19).

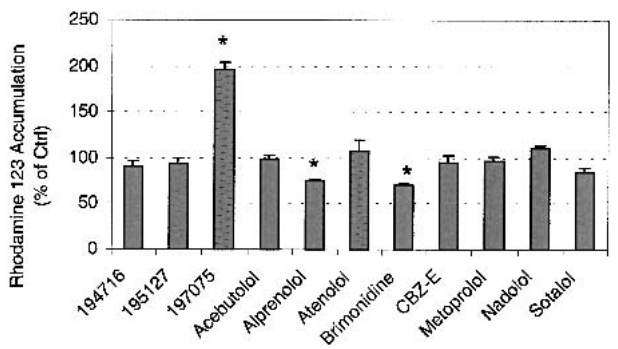

Fig. 6. Effect of test compounds (1 mM) on rhodamine 123 accumulation in TR-iBRB cells. Data are expressed as percent of control uptake (n = 4). Statistical significance is denoted by the asterisks.

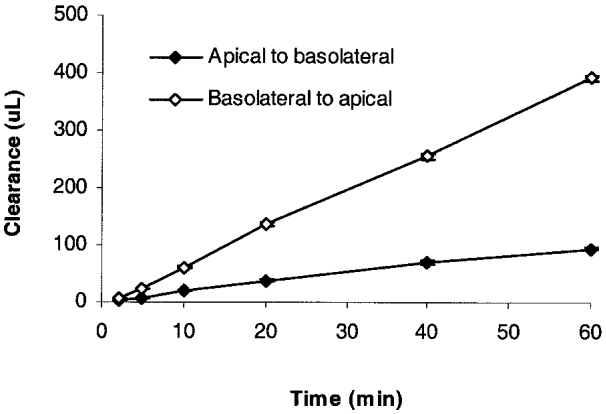

Fig. 7. Bidirectional transport of AGN 197075 (10 μM) across MDCK-MDR1 cell monolayers (TEER = 305 $\Omega \cdot cm^2$). P_{app} values were estimated at 2.38×10^{-5} cm/s and 9.79×10^{-5} cm/s for the apical to basolateral and the basolateral to apical directions, respectively.

Based on studies of paracellular permeability across cultured epithelial cell layers such as Caco-2 and MDCK cells, leakier cell layers with lower TEER values tend to have an increased contribution by paracelluar transport to the overall transport (21). In our TR-iBRB cell model, however, the more hydrophilic solute atenolol, which only crosses cell layers by paracellular diffusion (22) and has very limited permeability across the BBB *in vivo* (23), remained one of the least permeable compounds among all tested. Therefore, the leakiness in the TR-iBRB cell layer may not skew paracellular transport to an extent that renders this *in vitro* tool erroneous in predicting drug transport across the BRB.

Noticeably, 3-OMG, AGN 197075, and rhodamine 123 had estimated P_{app} values significantly deviating from those predicted by their cLogD values and hence were not included in constructing the linear relationship between P_{app} and cLogD in Fig. 4. Among the three, 3-OMG is a substrate for GLUT1, which exclusively mediates the sodium-independent D-glucose transport across the BRB and BBB to support and maintain normal metabolic activity in the brain and the retina (24). We observed higher 3-OMG permeability than that expected based on its cLogD value (Fig. 4). This is most likely a result of transport activities by GLUT1. The same observation was made for glucose permeability across the BBB measured by *in situ* perfusion in rats and mice, along with other substrates of transporter proteins expressed at the BBB including alanine and phenylalanine (20). Moreover, the permeability value for the P-gp substrate rhodamine 123 was significantly below the linear regression line (Fig. 4). This is a direct result of active efflux by P-gp, which was shown to be expressed in TR-iBRB cells when grown on filter membrane,

at a similar level as those grown in cell culture flask (Fig. 5). Again, similar observations were made for other P-gp substrates including vincristine, vinblastine, digoxin, and quinidine, when their permeability across the BBB was measured by either *in situ* perfusion in rats and mice or brain uptake in rats following intravenous injection (19,20).

In addition to rhodamine 123, AGN 197075 also stood out with significantly lower permeability than that predicted by its lipophilicity. Therefore, experiments were carried out to determine if it was a P-gp substrate. As shown in Fig. 6, AGN 197075 significantly inhibited P-gp–mediated efflux of rhodamine 123 out of the TR-iBRB cells, whereas all other compounds did not show such inhibition. Incidentally, these noninhibiting compounds had P_{app} values that correlated well with their lipophilicity (Fig. 4). Furthermore, AGN 197075 exhibited distinct directional transport across the MDR1-MDCK cell layer overexpressing human P-gp, favoring transport in the basolateral to apical direction. This result confirmed that AGN 197075 is a substrate for P-gp, as suggested by the transport data obtained from TR-iBRB cell layers.

Therefore, the cultured TR-iBRB cell layers not only differentiated compounds in their permeability with a correlation to their physicochemical properties, as observed *in vivo* and *in situ*, they were also able to distinguish compounds that are transported by active transporters present at the inner BRB. Some researchers have recommended the usage of cell lines such as MDCK and Caco-2 cells as *in vitro* tools for prediction of BBB permeability (25,26). Although these cell culture models can probably adequately predict and rank order compounds that passively diffuse across the barriers, they are not of the same origin as brain and retinal endothelial cells and would therefore lack the expression of active transporters unique to, or possess transporters that are absent in, these endothelial cells. For example, Lundquist *et al.* (27) compared *in vitro* permeability of 20 compounds of varying molecular weight across Caco-2 cells and across primary cultured bovine brain endothelial cells, to the *in vivo* brain uptake of the same compounds. Although a good correlation was observed between *in vivo* BBB penetration and *in vitro* permeability across brain endothelial cells, correlation of either to permeability across Caco-2 cells was much poorer. These observations illustrated the limitation of the Caco-2 cells, which might apply to other cell lines of non-CNS origin, to predict BBB permeability of compounds *in vivo*. In this regard, TR-iBRB cells derived from retinal endothelial cells would serve as a better model for the BRB *in vivo*, not only for passively transported compounds but also for those recognized and transported by active transporter proteins.

In conclusion, TR-iBRB cells, when grown on permeable membrane, provide a useful tool for predicting permeability across the BRB. The usefulness of this model for high throughput screening and rank ordering of drug candidates intended for the back of the eye in treatment of ocular diseases needs further characterization on correlation with *in vivo* data.

ACKNOWLEDGMENT

The authors wish to thank Dr. Ken-ichi Hosoya and Dr. Piet Borst for the TR-iBRB and the MDR1-MDCK cell lines used in this study.

REFERENCES

1. D. A. Infeld and J. G. O'Shea. Diabetic retinopathy. *Postgrad. Med. J.* **74**:129–133 (1998).
2. E. T. Cunningham Jr., R. D. Levinson, L. M. Jampol, R. E. Engstrom, Jr., H. Lewis, and G. N. Holland. Ischemic maculopathy in patients with acquired immunodeficiency syndrome. *Am. J. Ophthalmol.* **132**:727–733 (2001).
3. S. van Soest, A. Westerveld, P. T. de Jong, E. M. Bleeker-Wagemakers, and A. A. Bergen. Retinitis pigmentosa: defined from a molecular point of view. *Surv. Ophthalmol.* **43**:321–334 (1999).
4. J. Cunha-Vaz. The blood–ocular barriers. *Surv. Ophthalmol.* **23**: 279–296 (1979).
5. M. Shakib and J. G. Cunha-Vaz. Studies on the permeability of the blood–retinal barrier. IV. Junctional complexes of the retinal vessels and their role in the permeability of the blood–retinal barrier. *Exp. Eye Res.* **5**:229–234 (1966).
6. J. Greenwood. Characterization of a rat retinal endothelial cell culture and the expression of P-glycoprotein in brain and retinal endothelium *in vitro*. *J. Neuroimmunol.* **39**:123–132 (1992).
7. Y. S. Chang, L. L. Munn, M. V. Hillsley, R. O. Dull, J. Yuan, S. Lakshminarayanan, T. W. Gardner, R. K. Jain, and J. M. Tarbell. Effect of vascular endothelial growth factor on cultured endothelial cell monolayer transport properties. *Microvasc. Res.* **59**:265–277 (2000).
8. G. L. King, A. B. Berman, S. Bonner-Weir, and M. P. Carson. Regulation of vascular permeability in cell culture. *Diabetes* **36**: 1460–1467 (1987).
9. K. Hosoya, M. Tomi, S. Ohtsuki, H. Takanaga, M. Ueda, N. Yanai, M. Obinata, and T. Terasaki. Conditionally immortalized retinal capillary endothelial cell lines (TR- iBRB) expressing differentiated endothelial cell functions derived from a transgenic rat. *Exp. Eye Res.* **72**:163–172 (2001).
10. N. J. Abbott, C. C. Hughes, P. A. Revest, and J. Greenwood. Development and characterisation of a rat brain capillary endothelial culture: towards an *in vitro* blood–brain barrier. *J. Cell Sci.* **103**(Pt 1):23–37 (1992).
11. K. Takata, T. Kasahara, M. Kasahara, O. Ezaki, and H. Hirano. Ultracytochemical localization of the erythrocyte/HepG2-type glucose transporter (GLUT1) in cells of the blood–retinal barrier in the rat. *Invest. Ophthalmol. Vis. Sci.* **33**:377–383 (1992).
12. K. Hosoya, T. Kondo, M. Tomi, H. Takanaga, S. Ohtsuki, and T. Terasaki. MCT1-mediated transport of L-lactic acid at the inner blood–retinal barrier: a possible route for delivery of monocarboxylic acid drugs to the retina. *Pharm. Res.* **18**:1669–1676 (2001).
13. D. Z. Gerhart, R. L. Leino, and L. R. Drewes. Distribution of monocarboxylate transporters MCT1 and MCT2 in rat retina. *Neuroscience* **92**:367–375 (1999).
14. M. P. Dehouck, P. Jolliet-Riant, F. Bree, J. C. Fruchart, R. Cecchelli, and J. P. Tillement. Drug transfer across the blood–brain barrier: correlation between *in vitro* and *in vivo* models. *J. Neurochem.* **58**:1790–1797 (1992).
15. H. Franke, H. J. Galla, and C. T. Beuckmann. An improved low-permeability *in vitro*-model of the blood–brain barrier: transport studies on retinoids, sucrose, haloperidol, caffeine and mannitol. *Brain Res.* **818**:65–71 (1999).
16. H. E. de Vries, M. C. Blom-Roosemalen, A. G. de Boer, T. J. van Berkel, and D. D. Breimer. and J. Kuiper. Effect of endotoxin on permeability of bovine cerebral endothelial cell layers *in vitro*. *J. Pharmacol. Exp. Ther.* **277**:1418–1423 (1996).
17. P. J. Gaillard and A. G. de Boer. Relationship between permeability status of the blood–brain barrier and *in vitro* permeability coefficient of a drug. *Eur. J. Pharm. Sci.* **12**:95–102 (2000).
18. S. I. Rapoport, K. Ohno, and K. D. Pettigrew. Drug entry into the brain. *Brain Res.* **172**:354–359 (1979).
19. V. A. Levin. Relationship of octanol/water partition coefficient and molecular weight to rat brain capillary permeability. *J. Med. Chem.* **23**:682–684 (1980).
20. H. Murakami, H. Takanaga, H. Matsuo, H. Ohtani, and Y. Sawada. Comparison of blood–brain barrier permeability in mice and rats using *in situ* brain perfusion technique. *Am. J. Physiol. Heart Circ. Physiol.* **279**:H1022–H1028 (2000).
21. A. Adson, T. J. Raub, P. S. Burton, C. L. Barsuhn, A. R. Hilgers, K. L. Audus, and N. F. Ho. Quantitative approaches to delineate

paracellular diffusion in cultured epithelial cell monolayers. *J. Pharm. Sci.* **83**:1529–1536 (1994).
22. C. Hilgendorf, H. Spahn-Langguth, C. G. Regardh, E. Lipka, G. L. Amidon, and P. Langguth. Caco-2 versus Caco-2/HT29-MTX co-cultured cell lines: Permeabilities via diffusion, inside- and outside-directed carrier-mediated transport. *J. Pharm. Sci.* **89**:63–75 (2000).
23. P. Agon, P. Goethals, D. Van Haver, and J. M. Kaufman. Permeability of the blood–brain barrier for atenolol studied by positron emission tomography. *J. Pharm. Pharmacol.* **43**:597–600 (1991).
24. A. K. Kumagai. Glucose transport in brain and retina: implications in the management and complications of diabetes. *Diabetes Metab. Res. Rev.* **15**:261–273 (1999).
25. J. W. Polli, J. E. Humphreys, S. A. Wring, T. C. Burnette, K. D. Read, A. Hersey, D. Butina, L. Bertolotti, F. Pugnaghi, and C. J. Serabjit-Singh. A comparison of Madin-Darby canine kidney cells and bovine brain endothelial cells as a blood–brain barrier screen in early drug discovery. In M. Balls, A.-M. van Zeller, and M. E. Halder (eds), *Progress in the Reduction, Refinement and Replacement of Animal Experimentation,* Elsevier, Amsterdam, 2000, pp. 271–289.
26. C. Lohmann, S. Huwel, and H. J. Galla. Predicting blood–brain barrier permeability of drugs: Evaluation of different *in vitro* assays. *J. Drug Target.* **10**:263–276 (2002).
27. S. Lundquist, M. Renftel, J. Brillault, L. Fenart, R. Cecchelli, and M. P. Dehouck. Prediction of drug transport through the blood–brain barrier *in vivo*: A comparison between two *in vitro* cell models. *Pharm. Res.* **19**:976–981 (2002).